

## Morphology of Pores and Interfaces and Mechanical Behavior of Nanocluster-Assembled Silicon Nitride Ceramic

Rajiv K. Kalia, Aiichiro Nakano, Kenji Tsuruta, and Priya Vashishta

*Concurrent Computing Laboratory for Materials Simulations, Department of Physics and Astronomy and Department of Computer Science, Louisiana State University, Baton Rouge, Louisiana 70803*

(Received 20 May 1996)

Million atom molecular-dynamics simulations are performed to investigate the structure, dynamics, and mechanical behavior of cluster-assembled  $\text{Si}_3\text{N}_4$ . These solids contain highly disordered interfacial regions with 50% undercoordinated atoms. Systems sintered at low pressures have percolating pores whose surface morphologies are well characterized by two values of the roughness exponent, 0.46 and 0.86; these are close to the experimental values found by Bouchaud *et al.* for fracture surfaces. Results for elastic moduli are consistent with a three-phase model for heterogeneous materials. [S0031-9007(96)02209-0]

PACS numbers: 61.43.Bn, 61.46.+w

In recent years a great deal of progress has been made in synthesizing a wide variety of metals, alloys, and ceramics containing ultrafine microstructures in the range of a few nanometers [1–3]. The synthesis of these materials involves the generation and sintering of nanometer size clusters. Generally speaking, the physical properties of nanophase solids are superior to those of ordinary coarse-grained materials. For example, it has been found that nanophase metals are stronger and nanophase ceramics are more ductile than conventional metals and ceramics with the same constituents. While it has been speculated that these improvements are caused by the unusual structural characteristics of interfacial regions [2], there is very little quantitative understanding about the interfacial structure or its influence on physical properties of nanophase materials. Experiments have yet to provide information about the morphology of pores or the structure and dynamics of atoms in interfacial regions of nanophase materials. As far as modeling is concerned, to date there is very little work done on nanophase materials [4]. (This is due to the fact that atomistic simulations are computationally very demanding: A realistic simulation of a nanophase solid may require  $\sim 10^6$  atoms since each nanocluster itself consists of several thousand atoms.)

In this Letter we report the results of large scale (up to 1 085 616 atoms) molecular-dynamics (MD) simulations of nanocluster-assembled silicon nitride. (Being an excellent high-temperature ceramic,  $\text{Si}_3\text{N}_4$  is used in turbine engines, ball bearings, pressure sensors, and microelectronic devices.) We have investigated the structure and dynamics of atoms in interfacial regions, the distribution and morphology of pores, and the effect of consolidation on mechanical properties. The MD simulations are performed with effective two- and three-body interatomic potentials [5]. The two-body terms consist of steric repulsion among atoms, a charge-dipole interaction that takes into account the large electronic polarizability of nitro-

gen, and a screened Coulomb interaction due to charge transfer between Si and N. Three-body interactions take into account covalent effects through bond-bending and bond-stretching terms. To establish the validity of the interaction scheme, we compare the MD results with a variety of experimental measurements. We find the following: (i) The bond lengths and bond-angle distributions in crystalline and amorphous  $\text{Si}_3\text{N}_4$  are in excellent agreement with experiments [6], (ii) the positions and relative heights of the peaks in the static structure factor for amorphous  $\text{Si}_3\text{N}_4$  are in good agreement with neutron scattering measurements [7], (iii) the phonon density of states of crystalline  $\alpha\text{-Si}_3\text{N}_4$  agrees well with inelastic neutron scattering experiments [6], (iv) the specific heat of crystalline  $\alpha\text{-Si}_3\text{N}_4$  is in excellent agreement with experiments over a wide range of temperatures [8], and (v) the bulk modulus and Young's modulus along different directions in  $\alpha\text{-Si}_3\text{N}_4$  deviate less than 10% from the experimental values [9].

The nanophase  $\text{Si}_3\text{N}_4$  systems we have simulated involve either 1 085 616 or 129 920 atoms. In the first case the initial configuration consists of 108 clusters of diameter 60 Å [10], positioned randomly in a cubic box of length 288.49 Å (mass density 1.0 g/cc); the second system has 32 random clusters of diameter 45 Å. In both cases periodic boundary conditions are imposed and the equations of motion are integrated with the reversible multiple time-scale algorithm [11]. Using the variable-shape MD approach [12], we first thermalize the million-particle system at zero pressure and 2000 K for 40 ps (the MD time step is 2 fs). Subsequently this system is sintered at 2000 K under an external pressure of 1 GPa. The pressure is then increased to 5 GPa and the system is again well thermalized at 2000 K. The system is further consolidated at 2000 K by increasing the external pressure to 10 and then 15 GPa. Subsequently the systems at 1, 5, and 15 GPa are cooled to 1500, 1000, 700, and 300 K. At each temperature and pressure,

we thermalize the system for several thousand time steps. After reaching the room temperature, we gradually remove the pressure (this causes only a small decrease in the mass density). The final mass densities of the three systems, corresponding to pressures of 1, 5, and 15 GPa, are 2.24, 2.67, and 2.94 g/cc. Using similar heating and cooling schedules, we have obtained four other systems in which the constituent clusters are 45 Å in diameter. The average mass densities of these systems are 2.28, 2.64, 2.84, and 2.95 g/cc (corresponding to external pressures of 1, 5, 10, and 15 GPa).

Figure 1 shows the spatial distribution of pores in two systems (with 60 Å nanoclusters) at room temperature. The color plots are obtained by dividing the MD box into small voxels (size 5.5 Å) and then identifying empty voxels. The figure shows that the nanophase system with an average mass density of 2.24 g/cc has a large number of pores (shown in red), including a percolating pore. The system at 2.94 g/cc has mostly high-density regions (denoted by the black background, they have the same density as the  $\alpha$ -crystal) and small isolated pores.

To investigate the morphology of the percolating pore in the nanophase system at 2.24 g/cc, we calculate the height-height correlation function,  $G(\sigma)$ ,

$$G(\sigma) = \langle [h(x + x_0, y + y_0) - h(x_0, y_0)]^2 \rangle^{1/2};$$

$$\sigma = (x^2 + y^2)^{1/2}. \quad (1)$$

The results, shown in Fig. 2(a), are best fitted with the power law  $G(\sigma) \sim \sigma^\zeta$  and two values of the exponent  $\zeta$ —0.46 below a certain cross-over length ( $\sim 12$  Å) and 0.86 above the cross-over length.

The morphology of the percolating pore in nanophase  $\text{Si}_3\text{N}_4$  is very similar to that of fracture surfaces. The latter has drawn a great deal of attention in recent years. Recent experiments [13,14] have shown that fracture surfaces are self-affine, i.e., the height-height correlation function for fracture surfaces scales as  $\sigma^\zeta$ . For a variety

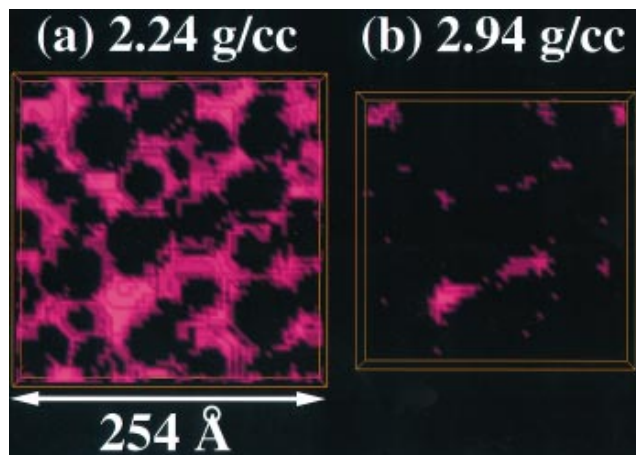


FIG. 1(color). Snapshots of pores (magenta) in 60 Å-thick slices of the 1085 616-particle nanophase system at mass densities 2.24 and 2.94 g/cc.

of brittle and ductile materials, the value of the roughness exponent  $\zeta$  is found to be close to 0.8. This observation has led to the conjecture that  $\zeta$  has a “universal” value, independent of the material or the mode of fracture (Måløy *et al.*, Ref. [13]). Recently Bouchaud and co-workers [15] carefully measured the roughness of fracture surfaces over a wide range of length scales. They find that the best fit to the data requires two roughness exponents—0.45 below a certain cross-over length and 0.84 above the cross-over length [9]. We have also investigated the crack-front morphology in fractured nanophase  $\text{Si}_3\text{N}_4$ . The results for the height-height correlation function, shown in the inset in Fig. 2(a), also obey the power-law relation  $G(\sigma) \sim \sigma^\zeta$  where  $\zeta$  is 0.5 below a certain cross-over length and 0.8 above the cross-over length.

We have also determined other structural characteristics of pores: the average radius, surface area, volume, and size distribution. These quantities are calculated by dividing the MD box into small voxels and then identifying pores by grouping contiguous empty voxels. The volume of a pore is simply the sum of the volumes of the empty voxels, and its surface area is the total area of all the faces which separate empty voxels on the pore surface from adjoining occupied voxels. The average pore radius is calculated from

$$R = \sqrt{\frac{1}{p} \sum_{i=1}^p |\mathbf{r}_i - \mathbf{r}_c|^2}, \quad (2)$$

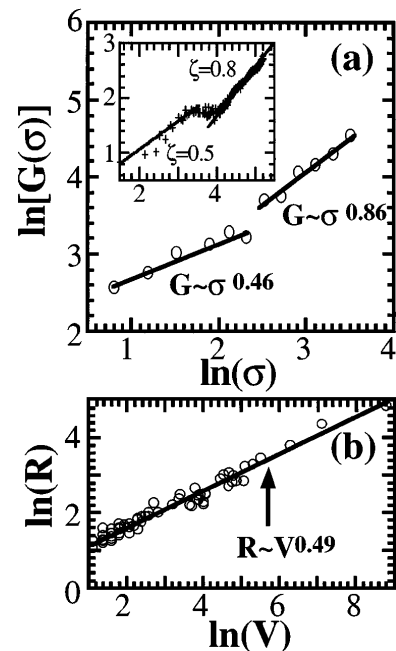


FIG. 2. (a) Height-height correlation function,  $G(\sigma)$ , for the percolating pore in the nanophase  $\text{Si}_3\text{N}_4$  at a mass density of 2.24 g/cc; for comparison, the corresponding results for the fractured surface in nanophase  $\text{Si}_3\text{N}_4$  are shown in the inset. (b) shows the dependence of the average pore radius ( $R$ ) on the pore volume ( $V$ ). Solid lines are best least-squares fits.

where  $\mathbf{r}_c$  is the pore center and  $\{\mathbf{r}_i\}$  are the centers of voxels on the pore surface. In Fig. 2(b) we have plotted  $R$  as a function of the average pore volume,  $V$ , on a log-log scale. For all the nanophase  $\text{Si}_3\text{N}_4$  systems we have studied, the radius  $R$  scales as  $V^\mu$  with  $\mu = 0.49 \pm 0.02$  and the fractal dimension,  $d = 1/\mu = 1.98 \pm 0.17$  [16].

We have also investigated in detail the structure of interfacial regions in nanophase  $\text{Si}_3\text{N}_4$ . Figure 3(a) shows Si-N pair-distribution function for particles inside the nanoclusters ( $g_{\text{Si-N}}^{(1)}$ ) and also for particles in interfacial regions ( $g_{\text{Si-N}}^{(2)}$ ). The sharp peaks in  $g_{\text{Si-N}}^{(1)}$  (dashed line) reflect the crystalline structure inside the nanoclusters. In interfacial regions, only the first peak in the pair-distribution function  $g_{\text{Si-N}}^{(2)}$  (solid line) is sharp; the second and third peaks are much broader than those in  $g_{\text{Si-N}}^{(1)}$ . The inset in Fig. 3(a) shows that the height of the first peak in  $g_{\text{Si-N}}^{(2)}$  is 4 times smaller than the height of the first peak in  $g_{\text{Si-N}}^{(1)}$  and that its position is shifted to a lower value relative to the position of the first peak in  $g_{\text{Si-N}}^{(1)}$ . Along with this shift, there is a decrease in the nearest-neighbor coordination of Si atoms in interfacial regions. As shown in Fig. 4, the average coordination in interfacial regions is close to 3.5 which implies that they have nearly the same number of three-fold and fourfold coordinated Si atoms (inside the nanoclusters the coordination of Si is four). Figures 3(b) and 3(c) show N-Si-N and Si-N-Si bond-angle distributions inside the nanoclusters (solid lines) and in interfacial regions

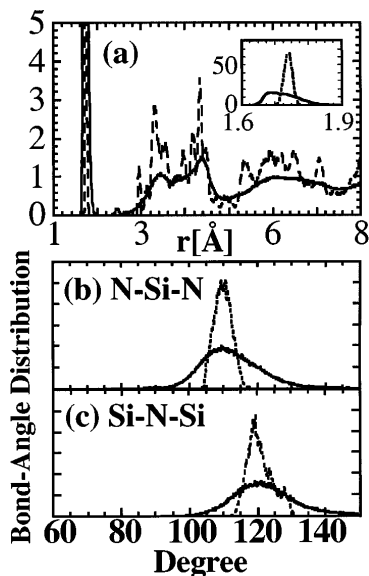


FIG. 3. Si-N pair-distribution functions (a) and bond-angle distributions [(b) and (c)] in the interior of nanoclusters (dashed lines) and in interfacial regions (solid lines) of the nanophase system with 1 085 616 particles at a mass density of 2.94 g/cc. The inset in (a) shows the first peaks in the pair-distribution functions.

(dashed lines). Clearly the latter are much broader and have smaller peaks than the distributions for the crystalline configuration. Thus, from partial pair-distribution functions and bond-angle distributions it is evident that interfacial regions in nanophase  $\text{Si}_3\text{N}_4$  are highly disordered. Atomic mean-square displacements indicate that atoms in interfacial regions are diffusing at 2000 K [17], which appears to be the primary mechanism of consolidation in nanophase  $\text{Si}_3\text{N}_4$ . Experiments indicate that this may be the dominant consolidation mechanism in other nanophase solids as well [2].

We have also investigated the effect of consolidation on elastic moduli of nanophase  $\text{Si}_3\text{N}_4$ . Figure 5 shows the porosity dependence of the bulk modulus,  $K$ , and the shear modulus,  $G$ . The open circles are the MD results for the bulk modulus of the three nanophase systems with 60 Å clusters; the open triangles and squares are the bulk and shear moduli, respectively, of systems with 45 Å clusters. The dependence of elastic moduli on porosity and cluster size can be understood in terms of a multicomponent model for heterogeneous materials [18]. According to this model, the bulk and shear moduli of a heterogeneous material are given by

$$\sum_{i=1}^n \frac{c_i}{1 - \alpha(1 - K_i/K)} = \sum_{i=1}^n \frac{c_i}{1 - \beta(1 - G_i/G)} = 1, \quad (3)$$

where  $n$  is the number of phases and  $c_i$ ,  $K_i$ , and  $G_i$  are their concentrations and bulk and shear moduli, respectively. The quantities  $\alpha$  and  $\beta$  are related to the Poisson's ratio,  $\nu$ , which in turn is determined by  $K$  and  $G$ ,

$$\alpha = \frac{1 + \nu}{3(1 - \nu)}; \quad \beta = \frac{2(4 - 5\nu)}{15(1 - \nu)}; \quad \nu = \frac{3K - 2G}{6K + 2G}. \quad (4)$$

In our nanophase systems we have three phases—pores, the interior crystalline regions of nanoclusters, and

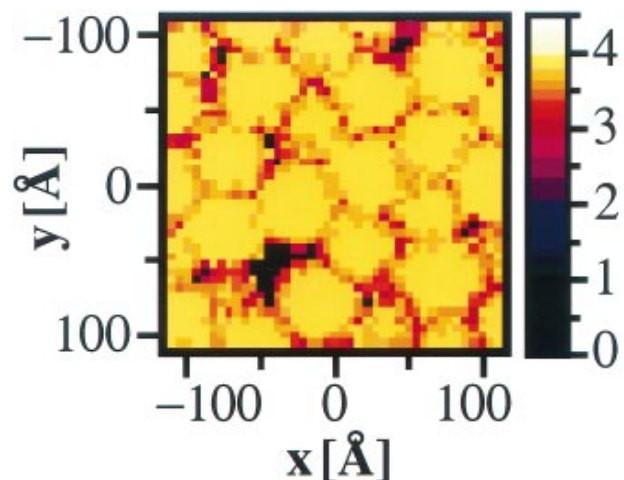


FIG. 4(color). Spatial distribution of the average Si coordination, projected onto the  $x$ - $y$  plane, in the nanophase system (with 1 085 616 particles) at 2.94 g/cc.

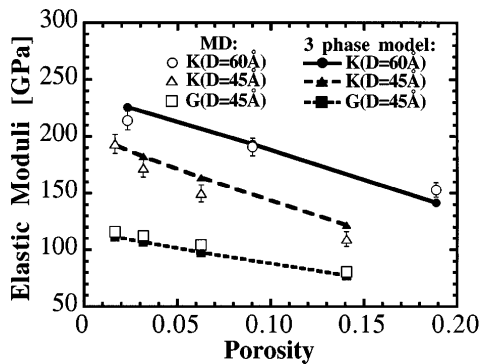


FIG. 5. Porosity dependence of the bulk modulus ( $K$ ) and shear modulus ( $G$ ). Open circles denote the MD results for bulk moduli of nanophase  $\text{Si}_3\text{N}_4$  with cluster size  $D = 60 \text{ \AA}$ ; open triangles and squares represent the MD results for bulk and shear moduli, respectively, of nanophase systems with  $45 \text{ \AA}$  clusters. Solid circles and triangles denote bulk moduli and solid squares represent shear moduli calculated from Eqs. 3 and 4. The solid, dashed, and dotted lines are drawn to guide the eye.

amorphous interfacial regions. The pore concentration,  $c_1$ , is the ratio of the pore volume to the total volume of the nanophase system; the concentration,  $c_2$ , is obtained from the effective volume of the crystalline part of nanoclusters; and the concentration of amorphous interfacial regions is determined from the condition,  $c_1 + c_2 + c_3 = 1$ . The bulk and shear moduli of individual phases are obtained from MD calculations for the  $\alpha$ -crystal and the amorphous  $\text{Si}_3\text{N}_4$  system (note,  $K_1 = G_1 = 0$ ): For the  $\alpha$ -crystal [9] we obtain  $K_2 = 289 \text{ GPa}$  and  $G_2 = 145 \text{ GPa}$  (this is an average over different directions); for the amorphous system we find  $K_3 = 181 \text{ GPa}$  and  $G_3 = 109 \text{ GPa}$ . Using these values of elastic moduli we solve Eqs. (3) and (4) for  $K$  and  $G$  [19], and in Fig. 5 we show these results by solid circles ( $K$ ), triangles ( $K$ ), and squares ( $G$ ). Clearly this three-phase model can successfully explain the MD results for the porosity dependence of elastic moduli. It also provides a simple explanation for the influence of the size of nanoclusters on elastic moduli. A nanophase solid with smaller clusters has a higher concentration of amorphous interfacial regions than a system with larger clusters because of greater surface-to-volume ratio. Since the elastic moduli of amorphous  $\text{Si}_3\text{N}_4$  are smaller than those for the  $\alpha$ -crystal, the nanophase system with smaller clusters ( $D = 45 \text{ \AA}$ ) will be less stiff than a nanophase system with larger clusters ( $D = 60 \text{ \AA}$ ).

In conclusion, large-scale MD simulations of nanophase  $\text{Si}_3\text{N}_4$  reveal the following: (i) Interfacial regions are amorphous and have 50% undercoordinated Si atoms, (ii) the fractal dimension of pores,  $d = 1.98 \pm 0.17$ , at all densities, (iii) systems sintered at low pressures ( $\sim 1 \text{ GPa}$ )

have percolating pores whose surface roughness exponents (0.46 and 0.86) are in excellent agreement with experiments [15], and (iv) the dependence of elastic moduli on porosity and grain size can be understood in terms of a three-phase model for heterogeneous materials [18].

This work was supported by DOE (Grant No. DE-FG05-92ER45477), NSF (Grant No. DMR-9412965), AFOSR (Grant No. F 49620-94-1-0444), and the Louisiana Education Quality Support Fund.

- [1] J. Karch, R. Birringer, and H. Gleiter, *Nature (London)* **330**, 556 (1987).
- [2] R. W. Siegel, in *Materials Interfaces: Atomic-Level Structure and Properties*, edited by D. Wolf and S. Yip (Chapman and Hall, London, 1992), p. 431; E. A. Stern *et al.*, *Phys. Rev. Lett.* **75**, 3874 (1995).
- [3] A. Pechenik *et al.*, *J. Am. Ceram. Soc.* **75**, 3283 (1992); V. P. Dravid *et al.*, *Nature (London)* **374**, 602 (1995).
- [4] Simulations have been done for metallic systems—see C.-L. Liu, J. B. Adams, and R. W. Siegel, *Nanostruct. Mater.* **4**, 265 (1994); H. Zhu and R. S. Averback, *Mater. Sci. Eng.* **204**, 96 (1995).
- [5] P. Vashishta *et al.*, *Phys. Rev. Lett.* **75**, 858 (1995).
- [6] C.-K. Loong *et al.*, *Europhys. Lett.* **31**, 201 (1995).
- [7] M. Misawa *et al.*, *J. Non-Cryst. Solids* **34**, 313 (1979).
- [8] *Silicon Nitride—1*, edited by S. Somiya *et al.*, (Elsevier Science, New York, 1990).
- [9] L. Cartz and J. D. Jorgensen, *J. Appl. Phys.* **52**, 236 (1981); A. Nakano *et al.*, *Phys. Rev. Lett.* **75**, 3138 (1995).
- [10] A spherical nanocluster of diameter  $60 \text{ \AA}$  was obtained from  $\alpha$ - $\text{Si}_3\text{N}_4$  crystal.
- [11] M. Tuckerman, B. J. Berne, and G. J. Martyna, *J. Chem. Phys.* **97**, 1990 (1992).
- [12] M. Parrinello and A. Rahman, *J. Appl. Phys.* **52**, 7182 (1981).
- [13] E. Bouchard *et al.*, *Europhys. Lett.* **13**, 73 (1990); *Phys. Rev. B* **48**, 2917 (1993); K. Måløy *et al.*, *Phys. Rev. Lett.* **68**, 213 (1992); **71**, 205 (1993).
- [14] V. Y. Milman *et al.*, *Phys. Rev. Lett.* **71**, 204 (1993); these measurements reveal a smaller value of the roughness exponent.
- [15] E. Bouchard and S. Navéos, *J. Phys. I (France)* **5**, 547 (1995).
- [16] D. Stauffer, *Introduction to Percolation Theory* (Taylor & Francis, London, 1985).
- [17] Self-diffusion constants of Si and N are estimated to be  $10^{-6} \text{ cm}^2/\text{s}$  at 2000 K.
- [18] B. Budiansky *J. Mech. Phys. Solids* **13**, 223 (1965).
- [19] In the model calculation  $\nu$  varies between 0.23 and 0.27. From MD calculations we obtain  $\nu = 0.27$  for the  $\alpha$ -crystal and the amorphous system at  $3.2 \text{ g/cc}$ . The experimental value for the  $\alpha$ -crystal is 0.22–0.28 (Ref. [8]).